

## Structural Investigation and Optical Properties of Silver Nanoparticles Synthesis by Chemical Method

J. Singh<sup>1,\*</sup>, J. Tripathi<sup>1</sup>, M. Sharma<sup>1</sup>, A. Valuskar<sup>1</sup>, G.S. Chandrawat<sup>1</sup>, S.N. Jha<sup>2</sup>, S. Tripathi<sup>2</sup>

<sup>1</sup> Department of Physics, ISLE, IPS Academy, Indore, Madhya Pradesh, India

<sup>2</sup> A&MPD, Bhabha Atomic Research Centre, Mumbai, India

(Received 10 February 2020; revised manuscript received 12 April 2020; published online 25 April 2020)

We reported here the synthesis, structural characterization and optical properties of silver nanoparticles (Ag NPs). Chemical synthesis method was used to synthesize the Ag NPs. Ethylene was used as capping and reducing reagent. As prepared Ag NPs sample was characterized by X-ray diffraction, X-ray absorption spectroscopy (XAS), scanning electron microscope (SEM) and fourier transform infrared spectroscopy (FTIR). Rietveld refinement of diffraction data revealed the dimensions of unit cell, hkl values, and Fm-3m space group of Ag NPs. The average crystallite size was found to be ~ 38.5 nm. Both X-ray absorption near edge structure (XANES) and Extended X-ray absorption fine structure (EXAFS) techniques at silver K-edge at BL-9 beam line at Indus-2 synchrotron radiation source (2.5 GeV, 125 mA), RRCAT, Indore (M. P.), India. A computer software package IFEFFIT was used to analyze physical parameters. FTIR revealed chemical bonding and symmetry of molecules.

**Keywords:** Nanoparticles, Chemical Method, XRD, FTIR, EXAFS.

DOI: [10.21272/jnep.12\(2\).02006](https://doi.org/10.21272/jnep.12(2).02006)

PACS numbers: 33.20.Rm, 33.20.Ea, 07. 85.Qe

### 1. INTRODUCTION

Metal nanoparticles have been of immense interest due to their unique features such as, optical [1], antibacterial [2] and catalytic properties [3]. Silver nanoparticles (AgNPs) have been widely studied for many decades due to their sole features and extensive range of applications. Their uses antibacterial activity [2, 4], biosensing [5] and imaging [6]. Among these applications, antibacterial activities have much attention because they potentially offer a solution to the problem of antibiotic resistance [7]. The silver was widely applied in wound treatment, medical devices, water purification, air treatment, cosmetics, aqueous paint etc. Along with the rapid development of nanotechnology, special attention has been focused on the Ag nanoparticles because of their exhibited stronger microbial activity and wider range of applications. Due to high electrical conductivity, the Ag nanoparticles are also applied in conductive inks, adhesives and pastes for variety of advanced electronic devices. In the present investigation the synthesis of Ag NPs by chemical route is discussed, which is an easy, simple and convenient route for preparing metal particles in nanometer range [8, 9]. The prepared silver nanoparticles were characterized using XRD, FT-IR SEM and EXAFS.

### 2. METHODS AND MATERIALS

#### 2.1 Materials and Synthesis of Ag Nanoparticles

The Silver nanoparticles were prepared by chemical method [9-13]. Initially 1.0 gram of silver acetate was mixed with 50 ml of ethylene glycol (EG) in a 100 ml 3-neck round bottle flask, equipped with condenser and thermometer. The chemical mixture was heated to 160 °C. The color of complex changed from off white to light grey and then finally nearly black after an inter-

val of about 1hr which indicates the initiation of formation of silver nanoparticles. The reaction was continued for another two hour. After the completion of the reaction the mixture was cooled to room temperature and sample was separated in the beaker by 50ml ethanol. Then, the obtained precipitate was washed with ultrasonic processor and 3-4 times by ethanol. After washing the precipitate the sample was dried at 60 °C and finally it was obtained in the form of dark grey powder. As prepared nanoparticles were used directly for the characterizations.

#### 2.2 Characterizations

The silver nanoparticles were characterized by XRD using Bruker D8 Advance X-ray diffractometer using (Cu K-alpha) 0.154 nm wavelength. The X-rays were detected using a fast counting detector based on Silicon strip technology (Bruker Lynx Eye detector). Further; the refinement was carried out through the profile matching routine of the FullProf 2000 software package. Morphology of synthesized AgNPs was characterized by scanning electron microscopy (SEM) (JEOL JSM 5600). A few micrograms of the nanoparticles of the sample were added to a fixed quantity of pure KBr and ground it systematically. Afterward, a pellet of the uniform mixture was made for this sample. The FTIR was obtained on a (Bruker, Germany, Vertex 70) instruments with the sample as KBR pellet in the wave number region of 400-4000 cm<sup>-1</sup>. X-ray absorption fine structure studies (EXAFS) at K-absorption edge of the silver nanoparticles. The results were recorded in the EXAFS beam line BL-9, synchrotron radiation source (2.5 GeV, 125 mA), RRCAT, Indore. Theoretical model has been generated from the available standard crystallographic database (COD-1100136) and was fitted with the experimental data.

\* [jaiveer24singh@gmail.com](mailto:jaiveer24singh@gmail.com)

### 3. RESULTS AND DISCUSSION

#### 3.1 Structural Characterization

Fig. 1 represents the XRD patterns of prepared Ag NPs sample.

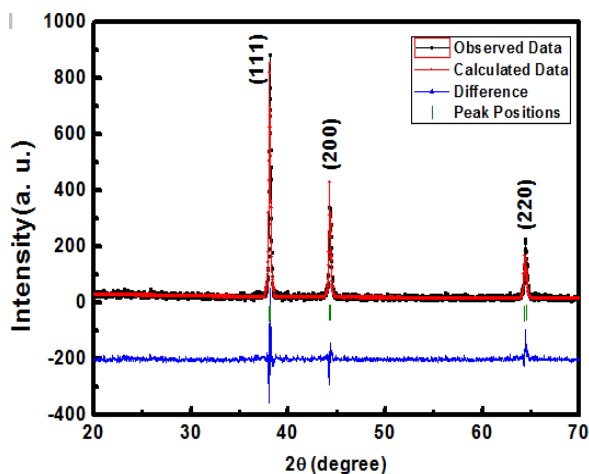


Fig. 1 – Structural Rietveld refinement of XRD patterns of Ag NPs

The peaks in the XRD spectra arising from corresponding Bragg's (hkl) planes for various diffraction positions were recorded as (111), (200) and (220) at  $2\theta$  values  $\sim 38.1^\circ$ ,  $44.26^\circ$  and  $64.44^\circ$  respectively, which indicates the Ag NPs are in crystalline FCC phase in nature with (JCPDS file # 04-0783) space group  $Fm\bar{3}m$  and determined Cell Parameter is  $4.089 \text{ \AA}$ . The broadening of Bragg's peak indicated the formation of nanoparticles. The sheerer relation [14] was used for the determination of average particle size ( $L$ )

$$L = \frac{0.9\lambda}{B\cos(\theta)},$$

where,  $\lambda$  is the incident X-ray wavelength,  $B$  = Full width at half maxima (FWHM) of the peak and  $\theta$  is the Bragg diffraction angle. The average particle size was determined  $\sim 38.5 \text{ nm}$ .

Further, Rietveld refinement was done by using FullProf 2000 software package. The pseudo-Voigt function was used to model the Bragg peaks. Corresponding fit values were found such as Profile Factor ( $R_p$ ) 66.4, Weighted Profile Factor ( $R_{wp}$ ) 45.4, Expected Weighted Profile Factor ( $R_{exp}$ ) 37, Bragg factor ( $R_B$ ) 8.67, Crystallographic  $R_F$  Factor 6.26 and  $\chi^2$  1.503 respectively.

#### 3.2 Scanning Electron Microscopy and Energy Dispersive X-Ray Analysis

Scanning Electron microscopy (SEM) techniques was used to analyze the surface morphology of the Ag NPs shown in Fig. 2. It was observed that all the particles have spherical-shape and aggregates into bigger particles with no well-defined morphology.

For the confirmation of formation of AgNPs EDAX study was used. The EDAX results were shown in (Fig. 3). EDAX results recorded for silver nanoparticles,

which showed a strong signal at 3 keV and few weak peaks were observed. Throughout the scanning range of binding energies, there is no peak to detect the impurity. This result indicated that the product was composed of high purity Ag nanoparticles.

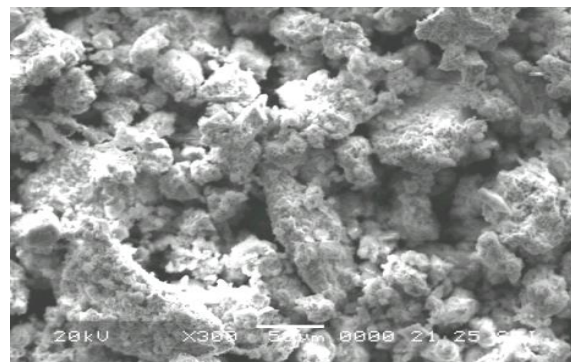


Fig. 2 – SEM image of Ag NPs

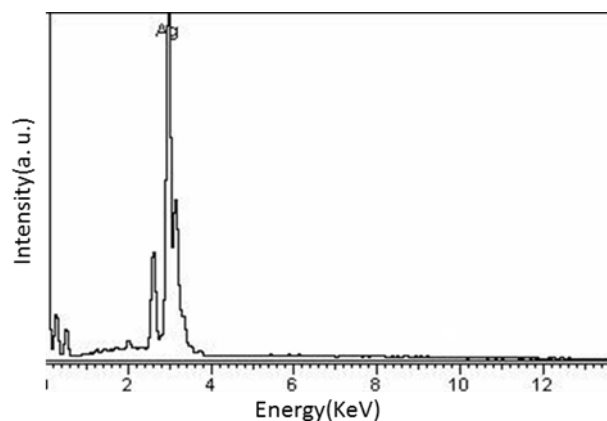


Fig.3 – EDAX spectra of Ag NPs

#### 3.3 Fourier Transform Infrared Spectroscopy

To find the ionic state of the Ag NPs, FTIR measurements were carried out to identify the potential functional groups of the molecules in the EG, which is responsible for the reduction of the silver ions.

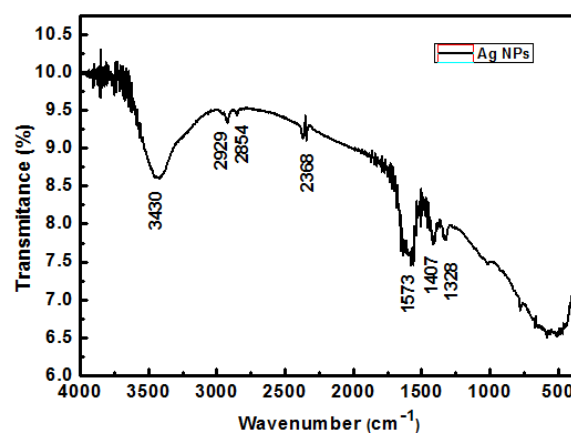


Fig. 4 – FTIR Spectra of Ag NPs

These functional molecules are associated with silver nanoparticles. FTIR spectra (Fig. 4) had shown that the band at  $3430 \text{ cm}^{-1}$  corresponds to N-H stretching

due to amines groups. The band at  $2929\text{ cm}^{-1}$ ,  $2854\text{ cm}^{-1}$  and  $2368\text{ cm}^{-1}$  are corresponds to O-H stretching of secondary alcohols. The band at  $1573.40\text{ cm}^{-1}$  corresponds to N-H bend amines. The transmittance peak at  $509\text{ cm}^{-1}$  corresponds to C-H bend alkenes. These observed peaks indicated that the carbonyl group formed amino acid residues capped on the surface of silver nanoparticles and reduces the particle size.

### 3.4 XAFS Study

If  $I_0$  and  $I$  were intensities obtained without and with placing the sample respectively in transmission mode then,  $I = I_0 e^{-\mu x}$ , where  $\mu(E)$  is absorption coefficient corresponding to the photon energy ( $E$ ) and  $x$  is the thickness of the absorber. The computer software package IFEFFIT was used to analyze the obtained experimental data. Synthesized AgNPs were characterized at Ag K-edge  $\sim 25514\text{ eV}$ . The spectrum obtained after characterization is shown in Fig. 5.

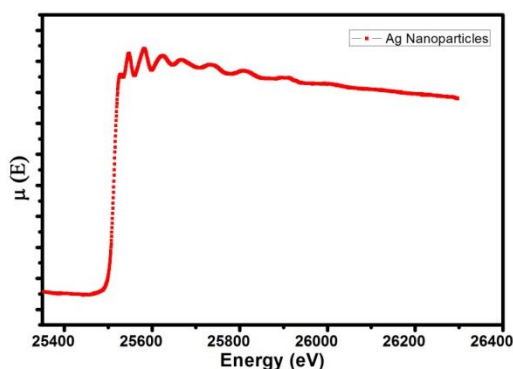


Fig. 5 – EXAFS spectrum of Ag nanoparticles

In X-ray absorption near-edge structure (XANES) region, ejected photoelectron probes the empty density of electronic states of the materials. As a result, XANES has long been known to be rich in chemical and structural information, short-range order around an absorbing element and can be Ag if Ag NPs are under investigation [13]. The normalized derivative spectra obtained from AgNPs is comparable with the normalized derivative spectra of standard Ag (metallic foil) obtained from *Hephaestus* computer Software package. This result is shown in Fig. 6.

Fig. 7 shows fitted Fourier Transform results in real space. Theoretical model was generated using the standard crystallographic data and fitted with the experimental results. The input parameter  $R_{bkg}$ , which decides the maximum frequency of the background, was set to  $1.0\text{ \AA}$ . Fourier transform was achieved over the  $k$ -range:  $k_{min} = 3\text{ \AA}^{-1}$ ,  $k_{max} = 7\text{ \AA}^{-1}$ . Data were fitted in the  $R$ -space by using  $k$ -weight 2 and fitting was carried out for coordination shells in the range  $1\text{ \AA}$ - $4\text{ \AA}$ . We used two scattering paths using FEFF calculations and R-factor was found to be good (0.006). The single value of passive electron reduction factor ( $S_0^2$ ) and energy shift for each path ( $\Delta E_0$ ) was used in both the scattering paths but different values of  $\Delta R$  guessed for both paths. Values obtained

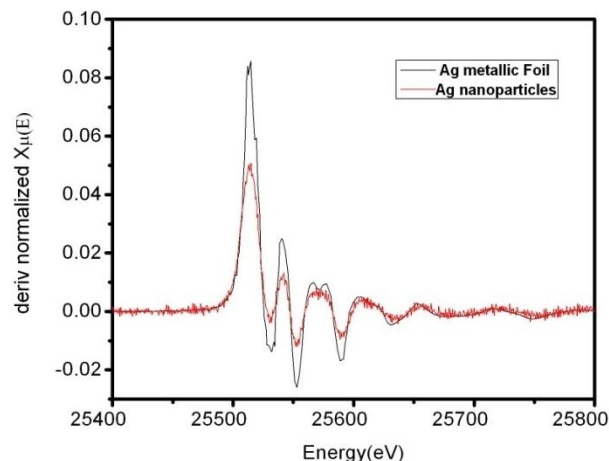


Fig. 6 – XANES results obtained from Hephaestus and Ag NPs

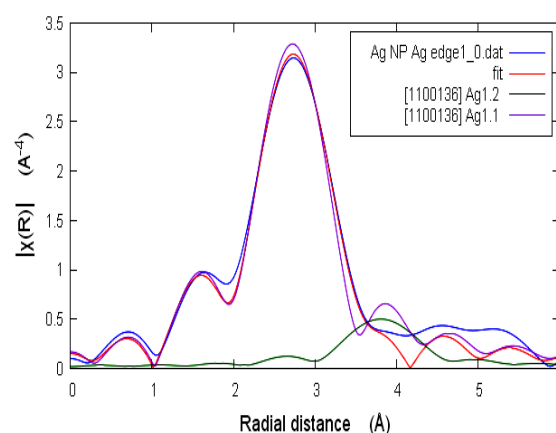


Fig. 7 – Magnitude of Fourier transform of the  $\chi(R)$  versus  $R$  curve

were in reasonable range ( $S_0^2 = 0.7$ ,  $\Delta E_0 = -1.7$ ). The Ag-Ag1.1 bridging distance was found to be  $2.86\text{ \AA}$  and Ag-Ag1.2 bridging distance was found to be  $4.08\text{ \AA}$  and in both scattering paths Debye factor ( $\sigma^2$ ) was found to be 0.01.

## 4. CONCLUSIONS

In outline, we have described a suitable method to synthesize the Ag NPs of average particle size  $38.5\text{ nm}$ . This synthesis method is much easier than other physical methods reported earlier and is very hopeful for the low-cost and large scale production of Ag NPs. It was found that Ag NPs have unique optical property, which, depend on the size and shape of the synthesized nanoparticles. The value of  $R$ -factor and passive electron reduction factor are reasonable good as reported earlier.

## AKNOWLEDGEMENTS

We would like to thank Dr. Mukul Gupta for XRD, Dr. U.P. Deshpande for FTIR and Mr. V.K. Ahire for SEM, UGC-DAE CSR, Indore and Dr. S.N. Jha for EXAFS RRCAT Indore for respective measurement.

## REFERENCES

1. E.A. Coronado, E.R. Encina, F.D. Stefani, *Nanoscale* **3**, 4042 (2011).
2. K.S. Siddiqi, *J. Trace Elem. Med. Bio.* **40**, 10 (2017).
3. N. Sharma, H. Ojha, A. Bharadwaj, D.P. Pathak, R.K. Sharma, *RSC Adv.* **5** No 66, 53381 (2015).
4. M. Rai, A. Yadav, A. Gade, *Biotechnol Adv.* **27** No 1, 76 (2009).
5. J.N. Anker, W.P. Hall, O. Lyandres, N.C. Shah, J. Zhao, R.P. Van Duyne, *Nat. Mater.* **7** No 6, 442 (2008).
6. K.S. Lee, M.A. El-Sayed, *J. Phys. Chem. B* **110** No 39, 19220 (2006).
7. M. Vanaja, G. Annadurai, *Appl. Nanosci.* **3**, 217 (2013).
8. J. Singh, N. Kaurav, K.K. Choudhary, G.S. Okram, *AIP Conf. Proc.* **1670**, 030034 (2015).
9. H. Wang, X. Qiao, J. Chen, S. Ding, *Colloid. Surface. A* **256** No 2-3, 111 (2005).
10. I.J. Godfrey, A.J. Dent, I.P. Parkin, S. Maenosona, G. Sankar, *J. Phys. Chem. C* **121**, 1957 (2017).
11. X.-F. Zhang, Z.-G. Liu, W. Shen, S. Gurunathan, *Int. J. Molec. Sci.* **17** No 9, 1534 (2016).
12. L. Gharibshahi, E. Saion, E. Gharibshahi, A. Shaari K. Matori, *Materials* **10** No 4, 402 (2017).
13. R.A. Davidson, D.S. Anderson, L.S.V. Winkle, K.E. Pinkerton, T. Guo, *J. Phys. Chem. A* **119**, 281 (2015).
14. S.G. Deshmukh, Vipul Kheraj, A.K. Panchal, *Mater. Today: Proc.* **5** No 10, 21322 (2018).